DOI:10.1158/0008-5472.CAN-12-2269

Cancer Research

Systems Analysis of BCL2 Protein Family Interactions Establishes a Model to Predict Responses to Chemotherapy

Andreas U. Lindner, Caoimhín G. Concannon, Gerhardt J. Boukes, et al.

Cancer Res 2013;73:519-528. Published online January 16, 2013.

DOI:10.1158/0008-5472.CAN-12-2269

Systems Analysis of BCL2 Protein Family Interactions Establishes a Model to Predict Responses to Chemotherapy

Andreas U. Lindner[1,2], Caoimhín G. Concannon[1,2], Gerhardt J. Boukes[1,2], Mary D. Cannon[2,5], Fabien Llambi[6], Deborah Ryan[2,3], Karen Boland[2,5], Joan Kehoe[1,3], Deborah A. McNamara[3], Frank Murray[5], Elaine W. Kay[4], Suzanne Hector[1,2], Douglas R. Green[6], Heinrich J. Huber[1,2], and Jochen H.M. Prehn[1,2]

Abstract

Apoptotic desensitization is a hallmark of cancer cells, but present knowledge of molecular systems controlling apoptosis has yet to provide significant prognostic insights. Here, we report findings from a systems study of the intrinsic pathway of apoptosis by BCL2 family proteins and clinical translation of its findings into a model with applications in colorectal cancer (CRC). By determining absolute protein quantifications in CRC cells and patient tumor samples, we found that BAK and BAX were expressed more highly than their antiapoptotic inhibitors. This counterintuitive finding suggested that sole inhibition of effector BAX and BAK could not be sufficient for systems stability in nonstressed cells. Assuming a model of direct effector activation by BH3-only proteins, we calculated that the amount of stress-induced BH3-only proteins required to activate mitochondrial apoptosis could predict individual death responses of CRC cells to 5-fluorouracil/oxaliplatin. Applying this model predictor to protein profiles in tumor and matched normal tissue samples from 26 patients with CRCs, we found that differences in protein quantities were sufficient to model the increased tumor sensitivity to chemotherapy compared with normal tissue. In addition, these differences were sufficient to differentiate clinical responders from nonresponders with high confidence. Applications of our model, termed DR_MOMP, were used to assess the impact of apoptosis-sensitizing dugs in lowering the necessary dose of state-of-the-art chemotherapy in individual patients. Together, our findings offer a ready clinical tool with the potential to tailor chemotherapy to individual patients. *Cancer Res; 73(2); 519–28. ©2012 AACR.*

Introduction

Most chemotherapeutics kill cancer cells by triggering programmed cell death or apoptosis (1). Perturbations in the apoptotic machinery contribute to carcinogenesis and are a major cause of chemo- and radiotherapy resistance (2). Hence, interindividual heterogeneity in tumor gene expression and protein profiles often limit the efficiency of standard-of-care, one size-fits-it-all chemotherapy paradigms. Therefore, patient-stratified treatment paradigms and dosage decisions are increasingly needed, requiring new tools that incorporate patient-specific, molecular data sets.

For stage II and III colorectal cancer (CRC), current treatment involves surgical resection followed by adjuvant therapy with genotoxic stress inducers oxaliplatin or irinotecan in combination with the antimetabolite 5-fluorouracil (5-FU; ref. 3). Genotoxic chemotherapeutics activate the BCL2 protein family–controlled process of mitochondrial outer membrane permeabilization (MOMP; refs. 4, 5). MOMP is executed by oligomerization of the proapoptotic BCL2 effector proteins BAK and BAX (6), which form pores in the mitochondrial outer membrane releasing apoptotic proteins that further activate caspase-dependent and -independent cell death pathways (4). In the absence of stress, BAK and BAX are inhibited by antiapoptotic BCL2 family proteins, including MCL1, BCL(X)L, and BCL2. Upon genotoxic stress and other stressors, a further apoptotic subclass of BCL2 proteins, the BH3-only proteins such as BID, BIM, and PUMA, are induced and derepress BAK and BAX from its inhibitors. Some BH3-only proteins may also activate BAK and BAX directly (7).

Several proteins involved in executing apoptosis prior or subsequent to MOMP, including BCL2 family members, have been proposed as molecular markers for cancer diagnosis and for patient stratification (8–11). However, the complexity of the interaction of antagonizing BCL2 family proteins makes it unlikely that mutations or deregulation of single apoptosis-related proteins are sufficient to characterize apoptosis execution or its impairment in patients. Therefore, holistic approaches studying the interplay of several proteins and including quantitative protein levels and interaction kinetics may be of significant interest (12–16). However, no model of

Authors' Affiliations: [1]Centre for Systems Medicine, [2]Department of Physiology and Medical Physics, Royal College of Surgeons in Ireland; Departments of [3]Surgery, [4]Pathology, and [5]Gastroenterology, Beaumont Hospital, Dublin, Ireland; and [6]Department of Immunology, St. Jude Children's Research Hospital, Memphis, Tennessee

Note: Supplementary data for this article are available at Cancer Research Online (http://cancerres.aacrjournals.org/).

Corresponding Authors: Jochen H.M. Prehn, Centre for Systems Medicine, Department of Physiology and Medical Physics, Royal College of Surgeons in Ireland, 123 St. Stephen's Green, Dublin 2, Ireland. Phone: 35314022255; Fax: 35314022447; E-mail: prehn@rcsi.ie; and Heinrich J. Huber, E-mail: heinhuber@rcsi.ie; Phone: 35314028538

doi: 10.1158/0008-5472.CAN-12-2269

DOI:10.1158/0008-5472.CAN-12-2269

BCL2 interaction and MOMP execution has yet been transferred into a clinical setting.

We here provide a computational systems model of MOMP regulation that integrates data on the interaction of pro- and antiapoptotic BCL2 proteins (17). By quantifying cell- and tissue-specific protein levels, the model developed allowed an assessment of the sensitivity of CRC cell lines to genotoxic stress and to differentiate patients with CRCs into clinical responders and nonresponders.

Materials and Methods

Patient cohort

Patient tissue was collected and stored from the Departments of Surgery, Gastroenterology, and Pathology, Beaumont Hospital, Dublin, Ireland. Tumor tissue was collected from 8 patients with stage II or 18 patients with stage III CRCs along with matched adjacent normal tissue. Clinical follow-up was obtained through a review of medical records by a clinical research nurse. Patients showing 4 years of disease-free survival were classified as favorable outcome and patients whose cancer recurred or who died from CRC as unfavorable outcome. Patients with hereditary forms of CRCs were excluded. Ethical approval was obtained by the Beaumont Hospital Ethics Committee, and informed consent was obtained from all patients. Tissue was stored as snap-frozen (−80°C) or in RNAlater (Ambion;−20°C). Tables 1 and 2 details the patient clinical characteristics and treatments.

Absolute protein quantifications

Patient tissue was lysed in 500 μL ice-cold buffer [50 mmol/L HEPES (pH 7.5), 150 mmol/L NaCl, 5 mmol/L Na-EDTA] and protease inhibitor (Sigma) and homogenized on ice. Samples were centrifuged at 14,000 × *g* for 10 minutes, supernatant collected and stored at −80°C. HeLa and CRC cell lysates were prepared similarly. For quantitative Western blotting, standard curves were constructed with varying concentrations (0.1–10.0 ng) of recombinant BAX (a kind gift from Prof. Christoph Borner), BAK (Abnova), BCL2 (R & D Systems), BCL(X)L (Abnova), and MCL1 (a kind gift from Prof. Christoph Borner), and varying concentrations (2–20 μg) of HeLa extract.

Western Blot images were acquired using a LAS-3000 Imager (FUJIFILM UK Ltd. Systems) and densitometry was conducted using ImageJ software. The intracellular concentration of each protein was calculated as previously described (14).

Briefly, Western blotting was conducted using different concentrations of recombinant proteins of BAK, BAX, BCL2, BCL(X)L, and MCL1. From these blots, a calibration curve was established for each protein, relating blot intensity to mass of loading (in μg; Fig. 3A). Subsequently, 20 μg of HeLa cell lysate was blotted and analyzed by densitometry. The total mass of

Table 1. Patient clinical characteristics

	Stage		
	II	III	II/III
Median age, y	73.5	63.0	
Gender			
Male	5	6	11
Female	3	12	15
Tumor location			
Cecal	0	4	4
Ascending colon	3	3	6
Transverse colon	1	1	2
Descending colon	1	1	2
Sigmoid	2	7	9
Rectosigmoid	0	2	2
Rectal	1	0	1
Median survival time, mo			
Disease free	19.5	20.0	20.0
Overall	28.0	20.0	20.0

Table 2. Details of the disease stage, chemotherapy treatment, and disease outcome for each of the 26 patients with CRCs within the study

Patient	Stage	Treatment	DFS	OS	Outcome
1	III	5-FU/Leu/Oxal	1	9	Unfavorable
2	III	5-FU/Leu			Favorable
3	III	None			Favorable
4	II	None			Favorable
5	III	5-FU/Leu			Favorable
6	II	None			Favorable
7	II	None			Favorable
8	III	5-FU/Leu	20	24	Unfavorable
9	III	5-FU/Leu			Favorable
10	III	5-FU/Leu			Favorable
11	III	5-FU/Leu			Favorable
12	III	5-FU/Leu/Oxal			Favorable
13	III	5-FU/Leu	16	20	Unfavorable
14	III	5-FU/Leu/Oxal	35		Unfavorable
15	III	5-FU/Leu			Favorable
16	III	5-FU/Leu/Oxal	45		Unfavorable
17	III	5-FU/Leu	4	14	Unfavorable
18	II	None			Favorable
19	II	None			Favorable
20	III	5-FU/Leu			Favorable
21	II	5-FU/Leu			Favorable
22	III	5-FU/Leu			Favorable
23	II	None	19	24	Unfavorable
24	II	None	20	32	Unfavorable
25	III	5-FU/Leu/Irin	18	20	Unfavorable
26	III	5-FU/Leu			Favorable

NOTE: Outcome was classified as favorable or unfavorable on the basis of disease recurrence/death within a 4-year period as described in Materials and Methods.

Abbreviations: DFS, disease-free survival within a 4-year period; Irin, irinotecan; Leu, leucovorin; none, no chemotherapy received; OS, overall survival within a 4-year period; Oxal, oxaliplatin.

DOI:10.1158/0008-5472.CAN-12-2269

the investigated proteins in the lysate was obtained from the calibration curves. Finally, assuming a HeLa cell volume of 3.1 pL (14) and the appropriate molecular weights for BAK, BAX, BCL2, BCL(X)L, and MCL1, cellular concentrations for these proteins were calculated (Fig. 3B).

Protein concentrations in the CRC cell lines and the patient samples were determined by comparison to signals from HeLa cell extracts as previously described (14, 18). Primary antibodies to MCL1 (1:250; BD Biosciences), BCL2 (1:100; Santa Cruz Biotechnology), BCL(X)L (1:250; Santa Cruz Biotechnology, Inc.), and β-actin (1:5,000; Sigma) were mouse monoclonal. Antibodies to BAK (1:250; Santa Cruz Biotechnology, Inc.) and BAX (1:1,000; Upstate Biotechnology) were rabbit polyclonal. The horseradish peroxidase (HRP)-conjugated secondary antibodies were from Jackson ImmunoResearch.

Mathematical model of stress dependency of MOMP

Absolute protein levels of the BCL2 family proteins BAK, BAX, BCL2, BCL(X)L, and MCL1 were used as model input and, therefore, were determined in the CRC cell lines Colo-205, HCT-116 (wild-type), HCT-116 *puma*$^{-/-}$, HCT-116 *p53*$^{-/-}$, HT-29, and LoVo, as well as in the patients' tumor and matched normal tissue. Expression of BCLW was not evident in any of the CRC cell lines or the patient-derived tissue. BH3-only proteins BAD, which is primarily regulated by AKT (19), or BMF, which plays a role in anoikis (20) but no predominant role in genotoxic stress (21) were disregarded. In the absence of genotoxic stress, no functional BH3-only proteins BIM, PUMA, and NOXA were assumed to be present.

Genotoxic stress was modeled to be p53-dependent and to involve the upregulation of the proapoptotic BH3-only proteins PUMA and NOXA (22). In addition, we modeled a FOXO3- (or E2F1-) dependent upregulation of BIM (23, 24). Production rates of all 3 proteins were assumed to be identical and modeled by a step function. Unless otherwise specified, production of BIM, PUMA, and NOXA was modeled to proceed at a constant rate until termination after 12 hours. The entire protein production over 12 hours was defined as (*protein*) *dose* η and used throughout the study as means to model stress severity. We considered an increased rate of MCL1 degradation upon genotoxic stress as shown previously (25) by modeling a drop of the MCL1 half-life from 45 to 17 minutes (Supplementary Table S2).

Protein production, degradation, and interactions were modeled by a pseudo-reaction network using mass action kinetics, translated into a set of ordinary differential equation (ODE) and solved using the MATLAB 7.3 (MathWorks, R2007b, 7.5.0.342) function *ode15s*. The detailed signaling pathways of the BCL2 family proteins are described in the Supplementary Modeling Details and Supplementary Tables S1–S7. Briefly, the antiapoptotic proteins BCL2, BCL(X)L, and MCL1 were modeled to bind to the proapoptotic proteins BIM, PUMA, and NOXA (and tBID wherever indicated) were modeled to be activated by BIM, PUMA, or tBID and to oligomerize unless they were inhibited by above antiapoptotic proteins. Effector homo-oligomers larger or equal to hexamers were considered as mitochondrial *pores* (26). MOMP was assumed to occur once 10% of the total effectors have formed pores as previously experimentally deducted (27). BH3-mimetics ABT-737 (28) and ApoG2 (29) were assumed to bind to and inhibit antiapoptotic proteins (Supplementary Table S6A), thereby facilitating apoptosis execution. To determine the *minimal BH3-only stress* to induce MOMP (Fig. 3–5), an iterative procedure was used. This procedure varied the protein dose in the model until the minimal *dose* η for which MOMP was achieved was determined within a range of 1.2×10^{-2} nmol/L. To test correlation of model predictions with survival of cell populations subsequent to administration of 5-FU/oxaliplatin, Pearson correlation analysis and Wilcoxon rank-sum were conducted using the MATLAB routines *corr* and *ranksum*. For the statistical analysis of the predicted stress *dose* η for the patients' tissue, as well as for analysis of patients outcome, the Wilcoxon signed an unsigned rank-sum test were conducted using the MATLAB routines *signrank* and *ranksum*. A separator of $\eta = 300$ nmol/L and the statistical software PASW (SPSS Inc., version 18) using the in-built log-rank test were used to test statistical independence between different Kaplan–Meier curves.

Qualitative analysis of activator and effector inhibition

As described in Llambi and colleagues (30), 2 tBID chimeras, $tBID^{BAK}$ and $tBID^{BAX}$, were considered where the BH3 domains of tBID were replaced by the BH3 domains of either BAK or BAX. $tBID^{BAK}$ and $tBID^{BAX}$ binding affinities to the antiapoptotic protein were modeled to be the same as for the protein (BAK or BAX) from where the BH3 domain was taken (Supplementary Table S7A). Activation kinetics of BAK and BAX by each chimera were taken from those of native tBID (Supplementary Table S4AB and S7B). A protein dose η of 1 μmol/L of either $tBID^{BAK}$ (B) and $tBID^{BAX}$ (C) was assumed with 500 nmol/L of BAK and no BAX (B) or cells with 500 nmol/L of BAX and no BAK (C). BCL2 or MCL1 were administered at specified doses. The maximum amount of BAK or BAX pores was calculated. The amount of pores in the area plots were normalized to 500 nmol/L.

Cell lines and culture

HCT-116 wt, *p53*$^{-/-}$, and *puma*$^{-/-}$ cells were obtained from Prof. Bert Vogelstein (Johns Hopkins University, Baltimore, MD). Colo-205, HT-29, and LoVo cells were obtained from Dr. Ken Nally (University College Cork, Cork, Ireland). The HeLa cells were purchased from the American Type Culture Collection (LGC Standards). The authenticity of the cell lines was confirmed by DNA STR profiling conducted by the DSMZ in October 2012. The genotype of the HCT-116 cells was verified by Western blotting. Colo-205, HeLa, and HCT-116 cells were maintained in RPMI-1640 supplemented with 10% fetal calf serum (FCS), 2 mmol/L L-glutamine, 100 U/mL penicillin, and 100 mg/mL streptomycin at 37°C in 5% CO_2. HT-29 and LoVo cells were grown in Dulbecco's Modified Eagle's Media (DMEM) supplemented with 10% FCS, 100 U/mL penicillin, and 100 mg/mL streptomycin.

Flow cytometry

Following treatments, cells were stained with Annexin V-FITC (Biovision) and propidium iodide (PI; Sigma) for 20

DOI:10.1158/0008-5472.CAN-12-2269

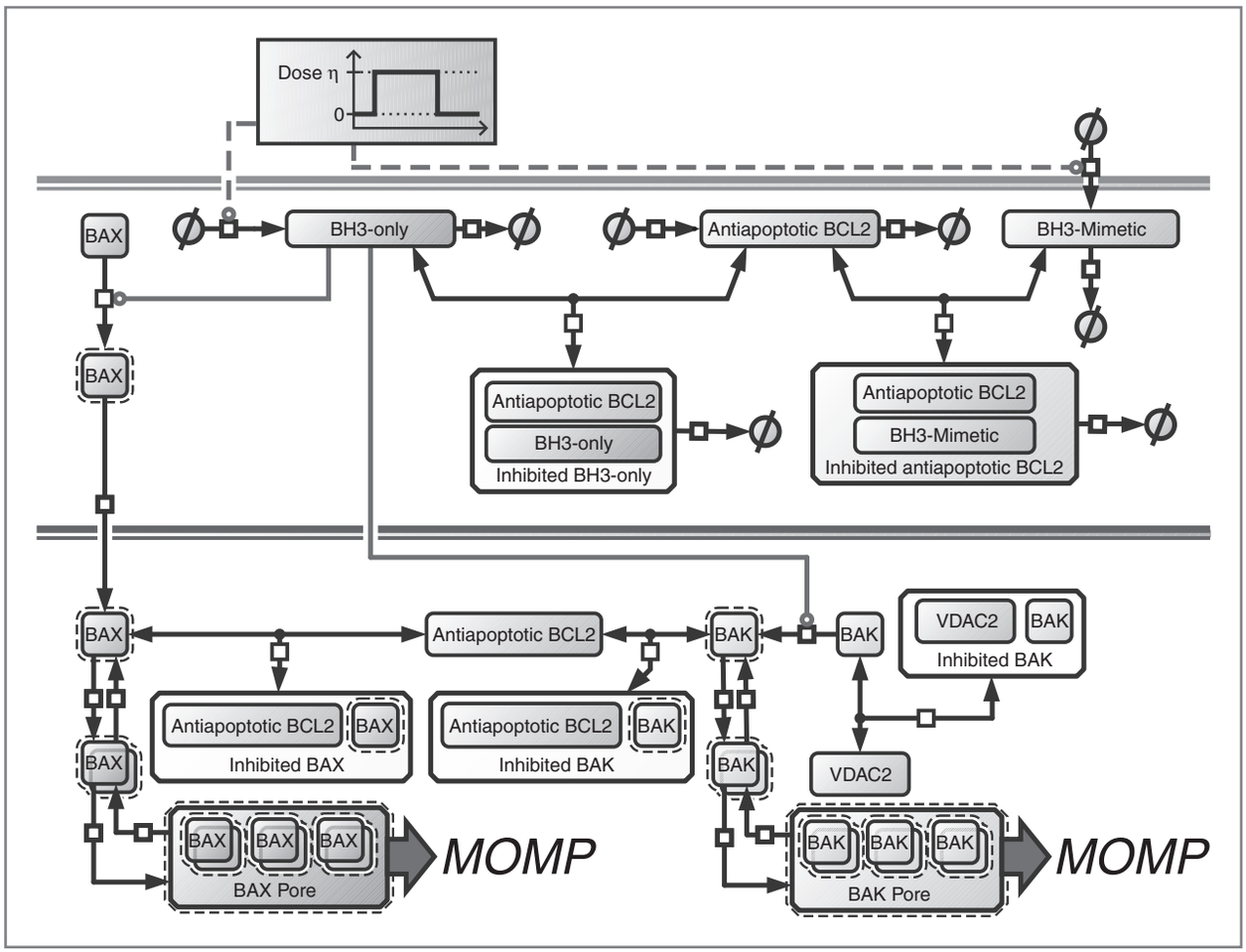

Figure 1. Model of BCL2 protein interaction during genotoxic stress. Systems biology graphical notation (SBGN) scheme of the computational model. The box labeled antiapoptotic BCL2 represents BCL2, BCL(X)L, and MCL1; the box labeled BH3-only indicates the genotoxic stress induced BH3-only proteins PUMA, NOXA, and BIM, whereas their heterodimers are described by the box labeled inhibited BH3-only. Active proteins are indicated with an additional dashed border. BH3-mimetic represents ABT-737 or ApoG2, which mimic the function of BH3-only proteins. The minimal amount of BH3-only proteins (*dose* η) for 10% effector homo-oligomerization (indicating MOMP) was subsequently calculated.

minutes at room temperature and analyzed using a CyFlow ML (Partec) flow cytometer and FloMax software. A minimum of 10,000 events were recorded for each sample.

Results

An *in silico* model for studying MOMP in response to genotoxic stress

We devised a computational model to study cellular BCL2 protein interaction and the process of MOMP in response to genotoxic stress (Fig. 1). We modeled genotoxic stress to induce the BH3-only proteins BIM, PUMA, and NOXA (31–33), whose expression levels we considered as surrogate of the chemotherapeutic dose and that lead to an interaction of pro- and antiapoptotic proteins resulting in effector (BAK and BAX) homo-oligomerization. MOMP was assumed to occur when homo-oligomers larger than or equal to hexamers (further denoted as pores; ref. 26) bound more than 10% of total effectors (12). The antiapoptotic proteins BCL2, BCL(X)L, and MCL1 were modeled to attenuate MOMP by engaging the BH3-only proteins and effectors. We modeled effector activation to require an activation step by PUMA or BIM. In the following section, we calculated the amount of effector pores under a given stress. Subsequently, we calculated and analyzed the minimum dose of BH3-only proteins necessary to induce MOMP (*dose* η in further, see Materials and Methods) in particular cells or patient tissues.

Systems modeling resembles experimental findings of two-step repression of MOMP

Every newly devised *in silico* model should be consistent with established qualitative and quantitative experimental data (12). Therefore, we investigated whether our model was able to reproduce the experimental findings of Llambi and colleagues (30). In this study, tBID chimeras, $tBID^{BAK}$ and $tBID^{BAX}$, were constructed whereby the BH3-domain of tBID was replaced with either those of BAK or BAX. Using the above model, we assumed an artificial cell line as described in Materials and Methods and resembled settings where

DOI:10.1158/0008-5472.CAN-12-2269

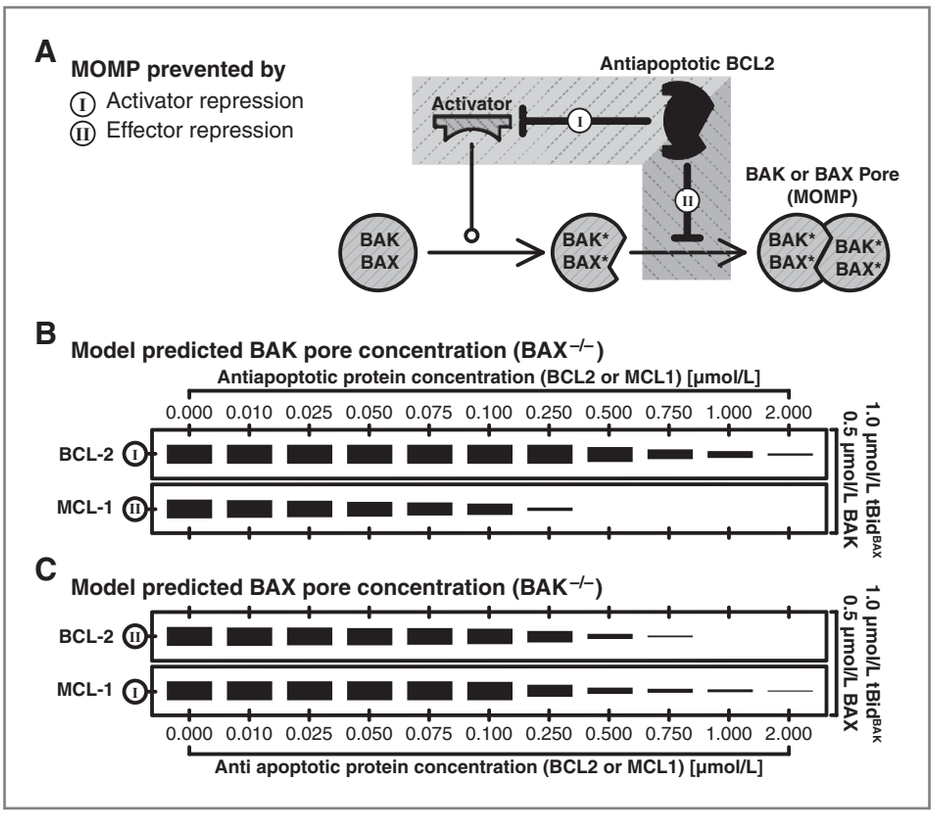

Figure 2. Model predicts effector repression to be more efficient than activator repression in inducing MOMP. Validation of the model based on the experimental data described in the work of Llambi and colleagues (30). A, models of activator and effector repression (I and II, respectively) are shown. B and C, area plots illustrating pore formation 96 hours after stress induction (normalized to an amount of 500 nmol/L of BAX or BAK). $BAX^{-/-}$ (B) or $BAK^{-/-}$ (C) cells were modeled to be subjected to 1 μmol/L of either a $tBID^{BAK}$ (B) or a $tBID^{BAX}$ (C) chimera over a 12-hour time period. The initial amounts of the antiapoptotic proteins BCL2 or MCL1 were varied as noted. Treatment of either $BAK^{-/-}$ cells with BCL2 or $BAX^{-/-}$ cells with MCL1 (both type II) required less antiapoptotic protein to prevent MOMP than treatment of either $BAX^{-/-}$ cells (expressing BAK; B) with BCL2 or $BAK^{-/-}$ cells (expressing BAX; C) with MCL1 (type I).

antiapoptotic proteins only inhibited the activator and not the effector (Fig. 2A, denoted as I). We implemented this by modeling $BAX^{-/-}$ cells (expressing BAK) to be exposed only to $tBID^{BAX}$ and BCL2 (binding to the $tBID^{BAX}$ and not to BAK) and by modeling $BAK^{-/-}$ cells (expressing BAX) to be exposed to $tBID^{BAK}$ and MCL1 (binding to $tBID^{BAK}$ and not BAX). In turn, effector repression (II) was investigated by assuming either BAX-deficient cells to be exposed to $tBID^{BAX}$ and MCL1 or BAK-deficient cells to be exposed to $tBID^{BAK}$ and BCL2. For all simulations, BCL(X)L was disregarded.

With these specific settings, we calculated the amount of BAK (or BAX) pores in $BAX^{-/-}$ (or $BAK^{-/-}$) cells in the presence of either only BCL2 or MCL1 and under different initial concentrations ranging from 0 to 2 μmol/L. Results for $BAX^{-/-}$ (Fig. 2B) and $BAK^{-/-}$ (Fig. 2C) cells are depicted by *in silico* area plots (in analogy to Fig. 4A; ref. 30) where the area of the bar is proportional to the calculated maximum amount of pores that is present during a period of 96 hours. In both cells types, less antiapoptotic protein is required to prevent pore formation when they bind to the effector (II) than when they bind to the activator (I), as shown by Llambi and colleagues (30).

The model predicted BH3-only stress dose η required for MOMP correlates with sensitivity of CRC cell lines to chemotherapeutic agents

Initial model calculations for HCT-116 and HeLa cells suggested that whether or not MOMP is induced upon the same genotoxic stress may depend on expression levels of BCL2 family members (Supplementary Fig. S1 and S2). We therefore determined absolute levels of BAK, BAX, BCL2, BCL(X)L, and MCL1 in the CRC cell lines Colo-205, HCT-116, HCT-116 *p53*$^{-/-}$, HCT-116 *puma*$^{-/-}$, HT-29, and LoVo (Fig. 3A–C and Supplementary Table S8). The expression of BCLW was not detectable in any of the cell lines investigated (data not shown; ref. 34). Likewise, expression of BFL-1/A1/BCL2A1 is mainly limited to cells of hematologic origin (35). Strikingly, despite cell line specific differences, most cell lines showed higher expression levels of BAK and BAX than total levels of the combined levels of the quantified antiapoptotic proteins (Fig. 3C). This striking result challenges the notion that apoptosis can be prevented by sole effector repression.

We investigated whether predictions of our model correlated to the susceptibility of different CRC cell populations to genotoxic stress. Apoptosis activation was quantified after treatment with 30 μg/mL of 5-FU and 10 μg/mL oxaliplatin for 48 hours. Cell death in the p53-mutated or -deficient cell lines was low (40%, 23%, and 20% for Colo-205, HCT-116 *p53*$^{-/-}$, and HT-29 cells), whereas 70% and 42% cell death was observed in the p53-competent cell lines, HCT-116 and LoVo, respectively. Cell death in HCT-116 *puma*$^{-/-}$ cells was 60%.

Next, we addressed whether our model was sufficient to account for the differential sensitivity to the chemotherapeutic agents. To identify a model predictor for cell death, we assumed that stress due to 5-FU/oxaliplatin treatment would induce expression of BIM, PUMA, and NOXA in p53- and PUMA-competent cells, expression of BIM in p53-mutated or

DOI:10.1158/0008-5472.CAN-12-2269

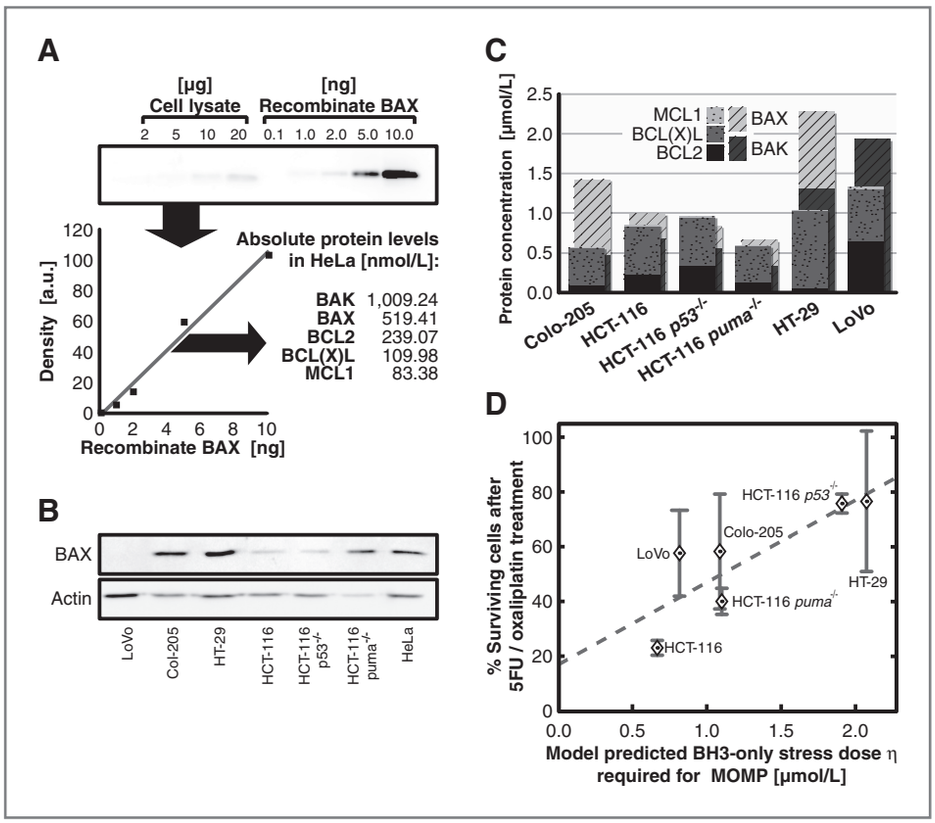

Figure 3. The required stress dose η is a predictor of cell sensitivity to undergo apoptosis after genotoxic stress. A and B, quantification of absolute BCL2 protein levels in CRCs and HeLa cells as exemplified for BAX. A, calibration curves relating blot intensity to protein mass of loading were constructed from Western blots using varying concentrations of purified BAX (0.1–10 ng). HeLa cell lysates were blotted and analyzed by densitometry on the same gel. The BAX concentration was obtained from the calibration curve. The intracellular concentration of each protein was calculated as previously (14). B, concentration of BCL2 family proteins was obtained relative to absolute concentrations in HeLa cells as determined in A. C, expression levels of BCL2 proteins of the given CRC cell lines. D, fraction of Annexin V and PI-negative cells after 48 hours treatment with 30 µg/mL of 5-FU and 10 µg/mL oxaliplatin were plotted against the *model predicted BH3-only stress dose*, η (Pearson coefficient = 0.84; $P = 0.04$), indicating a positive trend (dashed line; $R^2 = 0.70$).

-deficient cells, and expression of BIM only and NOXA in HCT-116 *puma*$^{-/-}$ cells. We next assumed that the *model predicted BH3-only stress* that is required to induce MOMP (*dose* η) in response to genotoxic stress in a typical cell would be a good predictor for the apoptosis susceptibility of a population. Results of our analysis are depicted in Fig. 3D. Indeed, *dose* η showed a positive correlation with cell survival, suggesting that a more sensitive cell population required less genotoxic stress in the model ($R^2 = 0.70$; Pearson coefficient = 0.84; $P = 0.04$).

The minimal stress-induced BH3-only protein dose η that is required for MOMP is a model predictor for tumor sensitivity and clinical outcome in CRC patients

As the model predicted *dose* η may represent a surrogate of the stress in a cell required for MOMP, we reasoned that it may also estimate the sensitivity of cells to chemotherapeutics. We obtained primary tumor and matched normal tissue for 8 patients with stage II and 18 patients with stage III CRCs with known clinical outcome (Tables 1 and 2). Patients with favorable outcome were defined as showing 4 years of disease-free survival, whereas unfavorable outcome were defined as patients showing recurrence or death from disease within 4 years.

We subsequently obtained absolute protein expressions of BCL2 proteins (Fig. 4A–C and Supplementary Table S9) from the resected tumor tissue and matched normal tissue and calculated the model predicted *dose* η that is needed to induce MOMP in the respective tissue. Strikingly, on average over all patients, our model predicted that tumor tissue required a significantly lower *dose* η (median value of 417 nmol/L) than cells from matched normal tissues (median of 764 nmol/L; $P < 0.0001$, Wilcoxon signed rank test; Fig. 4D), in agreement with other studies suggesting higher sensitivity of tumor tissue to apoptotic agents (36, 37). This finding may be consistent with the existence of a therapeutic window, defined as the difference in the predicted *dose* η between tumor and matched normal tissue, which the model allowed to be calculated for each patient individually (Supplementary Fig. S3).

We then compared the model predicted *dose* η for all 18 patients with favorable outcome and unfavorable outcome who received adjuvant 5-FU–based chemotherapy (Fig. 4E, Tables 1 and 2), as well as for all 26 patients, irrespective of whether or not they received chemotherapy after surgery (Fig. 4F). Of note, patients with 4-year disease-free survival were predicted to be more responsive to chemotherapeutic stimuli, as, indicated by the lower amount *dose* η, they required for MOMP (median of 191 vs. 566 nmol/L of *dose* η, respectively; $P = 0.0441$, Wilcoxon rank-sum test; Fig. 4E). Moreover, patients with overall favorable outcome also tended to be less resistant to stress-induced BH3-only protein induction than those with unfavorable outcome (median of 216 vs. 581 nmol/L of *dose* η, respectively; $P = 0.0523$, Wilcoxon rank-sum test; Fig. 4F).

We reckoned that a protein dose of 300 nmol/L may be a good separator to distinguish between patients with favorable

DOI:10.1158/0008-5472.CAN-12-2269

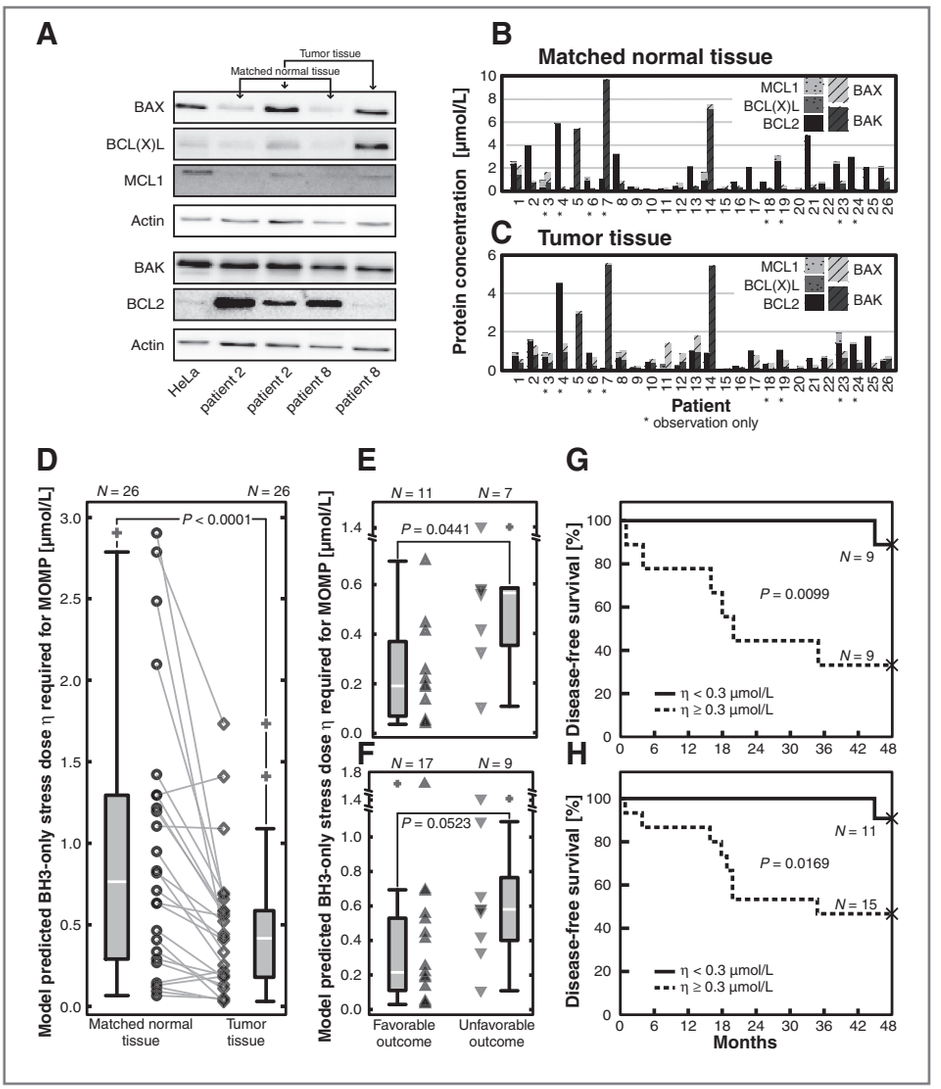

Figure 4. DR_MOMP can be used as predictor of clinical success in patients with CRCs. A, representative Western blot for BAX, BCL(X)L, MCL1, BAK, and BCL2 in tumor and matched normal tissue from patients with CRCs alongside the HeLa control. B and C, the given BCL2 family proteins were quantified in matched normal tissue (B) and tumor tissue (C) in 26 patients with stage II and III CRCs by quantitative Western blotting. D, model predicted BH3-only stress *dose* η required for MOMP was calculated for patient matched normal and tumor tissue. Matches are indicated by solid lines. Tumor tissue (right box plot) was predicted to require less *dose* η than the matched normal tissue (left box plot), consistent with the notion of cancer cells being primed to death (36, 37). Wilcoxon signed rank test confirmed significance between both groups ($P < 0.0001$). E and F, the calculated *dose* η can distinguish patients with favorable and unfavorable clinical outcome. Tumor tissue of 18 patients (E) who received adjuvant 5-FU–based chemotherapy and all 26 patients (F) were analyzed by the model. Patients were classified on the basis of disease-free survival within 4 years after surgery. Those patients with favorable clinical outcome required a significantly lower *dose* η than patients with unfavorable outcome. G and H, Kaplan–Meier curves of disease-free survival were generated for patients where the model predicted necessary *doses* $\eta < 0.3$ µmol/L or ≥ 0.3 µmol/L. Patients who required *doses* $\eta < 0.3$ µmol/L for MOMP (solid line) had a better outcome than those requiring *doses* η of ≥ 0.3 µmol/L (dashed line). Statistical independence of Kaplan–Meier curves between both groups were tested by log-rank test for patients who received adjuvant 5-FU–based chemotherapy (G; $P = 0.0099$) and for all patients (H; $P = 0.0169$).

or unfavorable outcome, as this dose lies in the middle of the medians of each group and, therefore, provided the optimal trade-off between specificity and sensitivity. Using this separator, Kaplan–Meier analysis of disease-free survival showed that patients with a predicted $\eta < 300$ nmol/L had a significantly longer survival than patients with $\eta \geq 300$ nmol/L ($P = 0.0099$ for prediction of response to chemotherapy; Fig. 4G; $P = 0.0169$, for overall outcome, Fig. 4H; log-rank test). Collectively, these results suggested that the increased sensitivity of tumor tissue compared with nontransformed cells may sufficiently be explained by differences in intra-individual protein profiles and that the modeled *BH3-only stress dose* η required for MOMP may be used as a prognostic marker and predictor of treatment responses to adjuvant chemotherapy. To indicate the potential of our model in aiding of dose response decisions for designing patient individual chemotherapy doses, we named the model *dose response medicinal outcome model predictor (DR_MOMP)*.

DOI:10.1158/0008-5472.CAN-12-2269

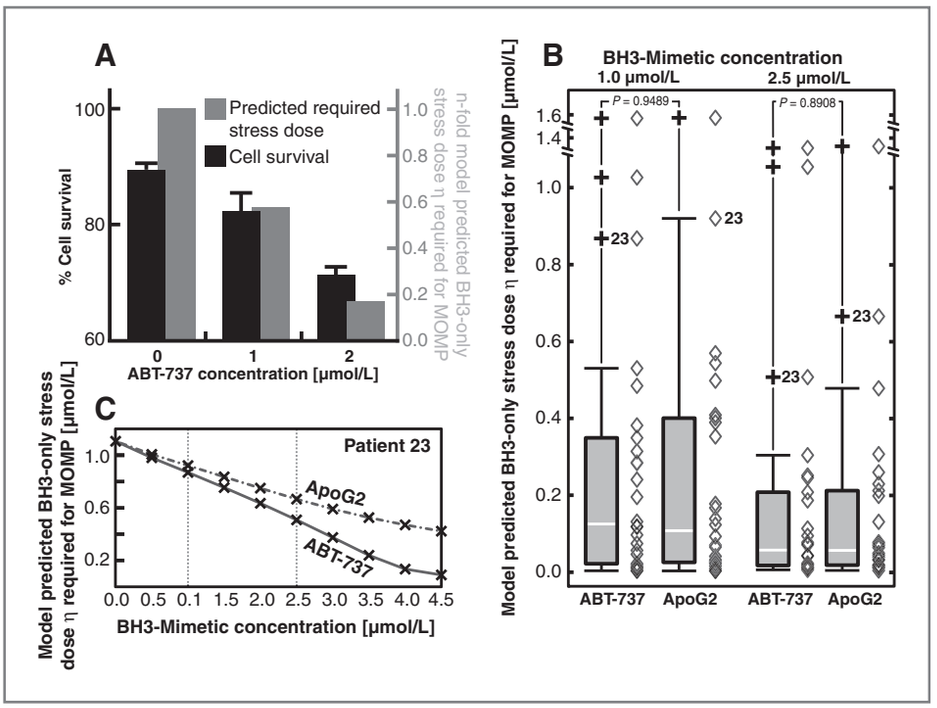

Figure 5. DR_MOMP as a tool to assess apoptosis sensitizers. Administration of either of the BH3-only mimetics ABT-737 or ApoG2 lowered the required *dose* η for chemotherapy. ApoG2 or ABT-737 was modeled to be administered over 12 hours. A, with increased ABT-737 concentrations, HT-29 cells became increasingly sensitized to treatment with 30 μg/mL 5-FU and 10 μg/mL oxaliplatin as observed by Annexin V/PI staining and subsequent flow cytometric analysis. This increased sensitivity was explained by *DR_MOMP* by a lower *dose* η. B and C, *dose* η was calculated for tumor tissue of the patients in Fig. 4. B, total administration of 1 μmol/L ABT-737 or ApoG2 within 12 hours decreased the necessary median *dose* η in tumor samples from patients ($n = 26$) from 417 nmol/L (Fig. 4D) to 109 (with ApoG2) or 126 nmol/L (with ABT-737). Administration of a higher dose of 2.5 μmol/L of both drugs did not markedly overall decrease the required dose for chemotherapy for all patients but decreased the variability in required dose between patients. C, *DR_MOMP* allowed assessment of patients with a different response to BH3-mimetics. As an example, in tumor tissue of patient 23, ABT-737 (solid line) reduced more significantly than ApoG2 (dashed dotted line).

DR_MOMP can be used as a tool for adjuvant and personalized therapies

BH3-mimetics are agents that are currently in clinical trial for adjuvant chemotherapy and sensitize cancer cells to apoptosis by mimicking the BH3 domain of BH3-only proteins (38). The synthetic drug ABT-737 (28) derepresses BH3-only activators by binding to BCL2 and BCL(X)L, whereas ApoG2 (29), albeit potentially also acting on glucose metabolism (39), sensitizes cells to apoptosis by binding to BCL2 and MCL1 (40). We implemented the molecular interactions governed by these drugs into *DR_MOMP* and carried out flow cytometric experiments of HT-29 cells treated with 5-FU/oxaliplatin in the absence or presence of ABT-737. Our results confirmed that ABT-737 increased the susceptibility of the cell populations to cell death in a dose-dependent manner. This increased susceptibility can be explained by *DR_MOMP* through a decreased *dose* η required for MOMP, suggesting that a lower dose of chemotherapy is required with increased ABT-737 concentrations (Fig. 5A).

We next investigated the effects of either ABT-737 or ApoG2 in individual patients. We modeled these administrations to lead to a total concentration of 1 or of 2.5 μmol/L of the respective drug over 12 hours (41) in the presence of 5-FU/oxaliplatin-based chemotherapy and again calculated the *dose* η that was required for *MOMP* in the patient tumor tissue. The median of *dose* η was reduced when both ABT-737 (from 417 to 126 nmol/L for 1 μmol/L and to 58 nmol/L for 2.5 μmol/L) and ApoG2 (to 109 and 58 nmol/L for 1 and 2.5 μmol/L) were applied (Fig. 5B). In both cases, we observed not only a decreased patient variability of the *dose* η with higher drug concentrations but also interindividual difference in the predicted responses to these 2 agents (Fig. 5C).

Discussion

Here, we investigated how the interactions of BCL2 family proteins translate different doses of chemotherapeutic stress into the all-or-none decision of MOMP. We established a model predictor acting as a surrogate for the chemotherapeutic dose required to induce cell death in tumor and matched normal tissues of individual patients. This model predictor correlated with the susceptibility of different cancer cell populations to stress, suggesting that cancer cells require less chemotherapeutic stress than nontransformed cells of the same patient (36, 37) and even was able to identify patients with favorable or unfavorable clinical outcome. Despite assuming that all tissues in all patients were unimpaired in expressing BH3-only proteins in response to chemotherapy, *DR_MOMP* robustly predicted patient outcome.

DOI:10.1158/0008-5472.CAN-12-2269

DR_MOMP may aid in predicting the optimal dose of chemotherapy that preserves healthy, normal tissue while killing cancer cells and predicting which patients respond to classical chemotherapy. It may also predict which patients may benefit from the addition of BH3-mimetics such as navitoclax (ABT-263), ABT-737, ApoG2, AT-101, or obatoclax, which are currently preclinically and clinically tested (38). We applied *DR_MOMP* to identify, in individual patients, how such mimetics may restore apoptosis by lowering the necessary dose of state-of-the-art chemotherapy. *DR_MOMP* suggested that the predicted effects of BH3-mimetics were patient specific. As patient heterogeneity is often a reason for failure in clinical trials (42, 43), *DR_MOMP* offers a possibility for *in silico* analysis of individual protein fingerprints from patients before administration of BH3-mimetics. As all mimetics target different protein interactions and as protein levels that mediate these interactions are patient specific, *DR_MOMP* may be able to predict the most suitable co-treatment, both in terms of type and concentration and may assist as an *in silico* tool in future phase II and III clinical trials. Our modeling also suggested that with sufficient concentrations of BH3-mimetics, the interindividual variability in predicted responses was significantly attenuated, indicating the potential of BH3-mimetics potential as future first-line treatment paradigms.

Input to *DR_MOMP* required absolute protein quantifications. We used quantitative Western blotting as opposed to alternatives such as ELISA as it allowed us to measure the signal of the protein of interest at its specific band and minimize the error due to unspecific antibody binding. However, for future clinical applications, array-based techniques such as reverse-phase protein arrays (RPPA; ref. 44) may provide a cost-effective and accurate alternative for higher numbers of proteins or specimens.

We have recently also developed a computational systems model to investigate apoptosis signaling subsequent to MOMP (14, 18) and showed that cancer cells have a decreased likelihood to undergo caspase activation than matched normal tissue (16, 18). Indeed, it is well established that caspase-inhibitory proteins such as X-linked inhibitor of apoptotic protein (XIAP) are overexpressed in cancer (45) and that caspase-activating proteins are inactivated through promoter methylation, chaperone binding, or phosphorylation (46). How can these results be reconciled with the present study? A higher "cancer cell sensitivity" to MOMP may indeed be associated with higher ability of cancer cells to adapt and respond to changes in their microenvironment, such as hypoxia/ischemia, reactive oxygen species production, and oncogene signaling. Cancer cells may accumulate tonic proapoptotic stimuli without committing MOMP and therefore require less chemotherapy to be "pushed over the edge." However, with MOMP as a potential all-or-none process, any information on dosage of genotoxic stress inducing chemotherapy and potentially any mitochondrial priming is likely to be lost after MOMP. Once a sufficient amount of stress is applied to induce MOMP, the decision whether or not apoptosis is executed may then depend on the expression levels of subsequent pro- and antiapoptotic players and potentially on bioenergetic parameters involved in this downstream process (14, 18, 47). It is therefore likely that through the analysis of both pathways independently, complementary model predictors for cancer cell survival or death can be established relating either to a dose-sensitive priming upstream to MOMP, or to a dose-independent, binary decision to evade of apoptosis execution downstream to MOMP.

Disclosure of Potential Conflicts of Interest

No potential conflicts of interest were disclosed.

Authors' Contributions

Conception and design: A.U. Lindner, C.G. Concannon, D.A. McNamara, F. Murray, E.W. Kay, D.R. Green, H.J. Huber, J.H.M. Prehn
Development of methodology: A.U. Lindner, D.A. McNamara, S. Hector, H.J. Huber
Acquisition of data (provided animals, acquired and managed patients, provided facilities, etc.): C.G. Concannon, G.J. Boukes, M.D. Cannon, D. Ryan, J. Kehoe, D.A. McNamara, S. Hector, H.J. Huber
Analysis and interpretation of data (e.g., statistical analysis, biostatistics, computational analysis): A.U. Lindner, C.G. Concannon, G.J. Boukes, M.D. Cannon, K. Boland, E.W. Kay, D.R. Green, H.J. Huber, J.H.M. Prehn
Writing, review, and/or revision of the manuscript: A.U. Lindner, C.G. Concannon, F. Llambi, F. Murray, E.W. Kay, S. Hector, D.R. Green, H.J. Huber, J.H.M. Prehn
Administrative, technical, or material support (i.e., reporting or organizing data, constructing databases): D.A. McNamara
Study supervision: D.A. McNamara, F. Murray, H.J. Huber

Acknowledgments

The authors thank Dr. Bert Vogelstein (Johns Hopkins University, Baltimore, MD) for *puma*- and *p53*-deficient HCT-116 cells and Dr. Christoph Borner (Albert Ludwigs University Freiburg, Freiburg, Germany) for recombinant proteins.

Grant Support

This research was supported by grants from the Health Research Board (APOCOLON; TRA/2007/26) to J.H.M. Prehn and E.W. Kay, Science Foundation Ireland (Investigator Award 08/IN.1/B1949) to J.H.M. Prehn and H.J. Huber, and the European Union FP7 (APO-SYS; 200767). M.D. Cannon was supported by a Higher Education Authority PRTLI Cycle 4-Clinician Scientist Fellowship award (F. Murray and J.H.M. Prehn).

The costs of publication of this article were defrayed in part by the payment of page charges. This article must therefore be hereby marked *advertisement* in accordance with 18 U.S.C. Section 1734 solely to indicate this fact.

Received June 13, 2012; revised October 8, 2012; accepted November 8, 2012; published online January 17, 2013.

References

1. Kaufmann SH, Earnshaw WC. Induction of apoptosis by cancer chemotherapy. Exp Cell Res 2000;256:42–9.
2. Pommier Y, Sordet O, Antony S, Hayward RL, Kohn KW. Apoptosis defects and chemotherapy resistance: molecular interaction maps and networks. Oncogene 2004;23:2934–49.
3. Goldberg RM, Sargent DJ, Morton RF, Fuchs CS, Ramanathan RK, Williamson SK, et al. A randomized controlled trial of fluorouracil plus leucovorin, irinotecan, and oxaliplatin combinations in patients with previously untreated metastatic colorectal cancer. J Clin Oncol 2004; 22:23–30.
4. Adams JM, Cory S. The Bcl-2 apoptotic switch in cancer development and therapy. Oncogene 2007;26:1324–37.
5. Hengartner MO. The biochemistry of apoptosis. Nature 2000;407: 770–6.

DOI:10.1158/0008-5472.CAN-12-2269

6. Wei MC, Zong WX, Cheng EH, Lindsten T, Panoutsakopoulou V, Ross AJ, et al. Proapoptotic BAX and BAK: a requisite gateway to mitochondrial dysfunction and death. Science 2001;292:727–30.
7. Leber B, Lin J, Andrews DW. Embedded together: the life and death consequences of interaction of the Bcl-2 family with membranes. Apoptosis 2007;12:897–911.
8. Hector S, Prehn JH. Apoptosis signaling proteins as prognostic biomarkers in colorectal cancer: a review. Biochim Biophys Acta 2009;1795:117–29.
9. Buglioni S, D'Agnano I, Cosimelli M, Vasselli S, D'Angelo C, Tedesco M, et al. Evaluation of multiple bio-pathological factors in colorectal adenocarcinomas: independent prognostic role of p53 and bcl-2. Int J Cancer 1999;84:545–52.
10. Manne U, Weiss HL, Grizzle WE. Bcl-2 expression is associated with improved prognosis in patients with distal colorectal adenocarcinomas. Int J Cancer 2000;89:423–30.
11. Sinicrope FA, Hart J, Michelassi F, Lee JJ. Prognostic value of bcl-2 oncoprotein expression in stage II colon carcinoma. Clin Cancer Res 1995;1:1103–10.
12. Huber HJ, Duessmann H, Wenus J, Kilbride SM, Prehn JH. Mathematical modelling of the mitochondrial apoptosis pathway. Biochim Biophys Acta 2011;1813:608–15.
13. Dussmann H, Rehm M, Concannon CG, Anguissola S, Wurstle M, Kacmar S, et al. Single-cell quantification of Bax activation and mathematical modelling suggest pore formation on minimal mitochondrial Bax accumulation. Cell Death Differ 2010;17:278–90.
14. Rehm M, Huber HJ, Dussmann H, Prehn JH. Systems analysis of effector caspase activation and its control by X-linked inhibitor of apoptosis protein. EMBO J 2006;25:4338–49.
15. Albeck JG, Burke JM, Aldridge BB, Zhang M, Lauffenburger DA, Sorger PK. Quantitative analysis of pathways controlling extrinsic apoptosis in single cells. Mol Cell 2008;30:11–25.
16. Schmid J, Dussmann H, Boukes GJ, Flanagan L, Lindner AU, O'Connor CL, et al. Systems analysis of cancer cell heterogeneity in caspase-dependent apoptosis subsequent to mitochondrial outer membrane permeabilisation. J Biol Chem 2012;287:41546–59.
17. Chen L, Willis SN, Wei A, Smith BJ, Fletcher JI, Hinds MG, et al. Differential targeting of prosurvival Bcl-2 proteins by their BH3-only ligands allows complementary apoptotic function. Mol Cell 2005;17:393–403.
18. Hector S, Rehm M, Schmid J, Kehoe J, McCawley N, Dicker P, et al. Clinical application of a systems model of apoptosis execution for the prediction of colorectal cancer therapy responses and personalisation of therapy. Gut 2012;61:725–33.
19. Datta SR, Dudek H, Tao X, Masters S, Fu H, Gotoh Y, et al. Akt phosphorylation of BAD couples survival signals to the cell-intrinsic death machinery. Cell 1997;91:231–41.
20. Puthalakath H, Villunger A, O'Reilly LA, Beaumont JG, Coultas L, Cheney RE, et al. Bmf: a proapoptotic BH3-only protein regulated by interaction with the myosin V actin motor complex, activated by anoikis. Science 2001;293:1829–32.
21. Ekoff M, Kaufmann T, Engstrom M, Motoyama N, Villunger A, Jonsson JI, et al. The BH3-only protein Puma plays an essential role in cytokine deprivation induced apoptosis of mast cells. Blood 2007;110:3209–17.
22. Villunger A, Michalak EM, Coultas L, Mullauer F, Bock G, Ausserlechner MJ, et al. p53- and drug-induced apoptotic responses mediated by BH3-only proteins puma and noxa. Science 2003;302:1036–8.
23. Hershko T, Ginsberg D. Up-regulation of Bcl-2 homology 3 (BH3)-only proteins by E2F1 mediates apoptosis. J Biol Chem 2004;279:8627–34.
24. Sunters A, Fernandez de Mattos S, Stahl M, Brosens JJ, Zoumpoulidou G, Saunders CA, et al. FoxO3a transcriptional regulation of Bim controls apoptosis in paclitaxel-treated breast cancer cell lines. J Biol Chem 2003;278:49795–805.
25. Kubota Y, Kinoshita K, Suetomi K, Fujimori A, Takahashi S. Mcl-1 depletion in apoptosis elicited by ionizing radiation in peritoneal resident macrophages of C3H mice. J Immunol 2007;178:2923–31.
26. Martinez-Caballero S, Dejean LM, Kinnally MS, Oh KJ, Mannella CA, Kinnally KW. Assembly of the mitochondrial apoptosis-induced channel, MAC. J Biol Chem 2009;284:12235–45.
27. Bleicken S, Classen M, Padmavathi PV, Ishikawa T, Zeth K, Steinhoff HJ, et al. Molecular details of Bax activation, oligomerization, and membrane insertion. J Biol Chem 2010;285:6636–47.
28. van Delft MF, Wei AH, Mason KD, Vandenberg CJ, Chen L, Czabotar PE, et al. The BH3 mimetic ABT-737 targets selective Bcl-2 proteins and efficiently induces apoptosis via Bak/Bax if Mcl-1 is neutralized. Cancer Cell 2006;10:389–99.
29. Laughton MJ, Halliwell B, Evans PJ, Hoult JR. Antioxidant and pro-oxidant actions of the plant phenolics quercetin, gossypol and myricetin. Effects on lipid peroxidation, hydroxyl radical generation and bleomycin-dependent damage to DNA. Biochem Pharmacol 1989;38:2859–65.
30. Llambi F, Moldoveanu T, Tait SW, Bouchier-Hayes L, Temirov J, McCormick LL, et al. A unified model of mammalian BCL-2 protein family interactions at the mitochondria. Mol Cell 2011;44:517–31.
31. Nakano K, Vousden KH. PUMA, a novel proapoptotic gene, is induced by p53. Mol Cell 2001;7:683–94.
32. de Bruijn MT, Raats DA, Hoogwater FJ, van Houdt WJ, Cameron K, Medema JP, et al. Oncogenic KRAS sensitises colorectal tumour cells to chemotherapy by p53-dependent induction of Noxa. Br J Cancer 2010;102:1254–64.
33. Happo L, Cragg MS, Phipson B, Haga JM, Jansen ES, Herold MJ, et al. Maximal killing of lymphoma cells by DNA damage-inducing therapy requires not only the p53 targets Puma and Noxa, but also Bim. Blood 2010;116:5256–67.
34. O'Reilly LA, Print C, Hausmann G, Moriishi K, Cory S, Huang DC, et al. Tissue expression and subcellular localization of the pro-survival molecule Bcl-w. Cell Death Differ 2001;8:486–94.
35. Vogler M. BCL2A1: the underdog in the BCL2 family. Cell Death Differ 2012;19:67–74.
36. Certo M, Del Gaizo Moore V, Nishino M, Wei G, Korsmeyer S, Armstrong SA, et al. Mitochondria primed by death signals determine cellular addiction to antiapoptotic BCL-2 family members. Cancer Cell 2006;9:351–65.
37. Ni Chonghaile T, Sarosiek KA, Vo TT, Ryan JA, Tammareddi A, Moore Vdel G, et al. Pretreatment mitochondrial priming correlates with clinical response to cytotoxic chemotherapy. Science 2011;334:1129–33.
38. Lessene G, Czabotar PE, Colman PM. BCL-2 family antagonists for cancer therapy. Nat Rev Drug Discov 2008;7:989–1000.
39. Olgiati KL, Toscano WA Jr. Kinetics of gossypol inhibition of bovine lactate dehydrogenase X. Biochem Biophys Res Commun 1983;115:180–5.
40. Wei J, Kitada S, Rega MF, Stebbins JL, Zhai D, Cellitti J, et al. Apogossypol derivatives as pan-active inhibitors of antiapoptotic B-cell lymphoma/leukemia-2 (Bcl-2) family proteins. J Med Chem 2009;52:4511–23.
41. Vogler M, Weber K, Dinsdale D, Schmitz I, Schulze-Osthoff K, Dyer MJ, et al. Different forms of cell death induced by putative BCL2 inhibitors. Cell Death Differ 2009;16:1030–9.
42. DiMasi JA, Feldman L, Seckler A, Wilson A. Trends in risks associated with new drug development: success rates for investigational drugs. Clin Pharmacol Ther 2010;87:272–7.
43. Rubin EH, Gilliland DG. Drug development and clinical trials–the path to an approved cancer drug. Nat Rev Clin Oncol 2012;9:215–22.
44. Hennessy BT, Lu Y, Gonzalez-Angulo AM, Carey MS, Myhre S, Ju Z, et al. A technical assessment of the utility of reverse phase protein arrays for the study of the functional proteome in non-microdissected human breast cancers. Clin Proteomics 2010;6:129–51.
45. Krajewska M, Kim H, Kim C, Kang H, Welsh K, Matsuzawa S, et al. Analysis of apoptosis protein expression in early-stage colorectal cancer suggests opportunities for new prognostic biomarkers. Clin Cancer Res 2005;11:5451–61.
46. Hanahan D, Weinberg RA. Hallmarks of cancer: the next generation. Cell 2011;144:646–74.
47. Huber HJ, Dussmann H, Kilbride SM, Rehm M, Prehn JH. Glucose metabolism determines resistance of cancer cells to bioenergetic crisis after cytochrome-c release. Mol Syst Biol 2011;7:470.